

IHEP-TH-98-02  
 AMES-HET-98-04  
 TU-546  
 hep-ph/9804343

## Probing Anomalous Top Quark Couplings At $e\gamma$ Colliders

Jun-Jie Cao<sup>1,2</sup>, Jian-Xiong Wang<sup>1</sup>, Jin Min Yang<sup>3</sup>, Bing-Lin Young<sup>4</sup> and Xinmin Zhang<sup>5,1</sup>

<sup>1</sup>*Institute of High Energy Physics, Academy Sinica,  
 Beijing 100039, China*

<sup>2</sup>*Department of Physics, Henan Normal University,  
 Xinxiang, Henan 453002, China*

<sup>3</sup>*Department of Physics, Tohoku University, Sendai 980-8578, Japan*

<sup>4</sup>*Department of Physics and Astronomy, Iowa State University,  
 Ames, Iowa 50011, USA*

<sup>5</sup>*CCAST (World Laboratory), P.O.Box 8730, Beijing 100080, China*

### ABSTRACT

We study in the effective Lagrangian approach the possibility of probing anomalous top quark charged current couplings in the single top production at a high energy  $e\gamma$  collider. We analyzed all possible dimension-six CP-conserving operators which can give rise to an anomalous  $Wtb$  coupling which represent new physics effect generated at a higher energy scale. For those operators which also give rise to anomalous  $Zb\bar{b}$  or right-handed  $Wtb$  couplings, we find that they are strongly constrained by the existing  $R_b$  and  $b \rightarrow s\gamma$  data. As a result, a collider with a luminosity of the order of  $100 \text{ fb}^{-1}$  is required to observe the anomalous effects. For other operators which currently subject to no strong constraints, the high energy  $e\gamma$  collider can probe their couplings effectively because of the clean environment of such a collider.

PACS: 14.65.Ha, 12.60.Cn

# 1. Introduction

The standard model (SM) has been proved to be phenomenologically successful. However, it is also generally believed that the SM will be augmented by new physics at higher energy scales. It is a challenge to search for ways to reveal the new physics effects at either the existing accelerators or the possible future ones. The top quark, because of its large mass, is believed to be more sensitive to new physics than other particles [1][2]. Hence, if anomalous top quark couplings exist, they may readily manifest themselves in the processes of top quark production and decay, and they may also affect the decay width of  $Z$  to  $b\bar{b}$  and  $b$  decays.

To probe the anomalous  $Wtb$  coupling, the single top quark production  $e\gamma \rightarrow t\bar{b}\nu$  at a high energy  $e\gamma$  collider has been analyzed in [3][4]. It was argued that because of the low background events, the top quark coupling  $Wtb$  can be measured with high precision, much better than in hadron colliders, the Tevatron and LHC. Therefore, more sensitive tests of the  $Wtb$  can be achieved in an  $e\gamma$  collider. In these early works, the probing of the  $Wtb$  coupling was done in isolation, its possible relations to other couplings and, therefore, possible constraints were not taken into account.

In this paper we re-examine the possibility of probing anomalous  $Wtb$  at an  $e\gamma$  collider in a more structured theoretical framework in which other couplings will come into play. We pay special attention to the effects of the latter and analyze the experimental constraints from  $R_b$  at LEP I and the experimental data on  $b \rightarrow s + \gamma$  at CESR. Presently the experimental data on  $R_b$  is consistent with the prediction of the standard model within  $1.4\sigma$ [5], which may in turn put strong bounds on some of the anomalous couplings of the top quarks.

A systematic, model independent framework for exploring anomalous top quark couplings is the effective Lagrangian. It introduces no new particles and can be made to deviate from the SM very slightly as required by the current data. There are two common approaches to the effective Lagrangian of the top quarks in the literature. They are formulated in terms of either the non-linear or linear realization of the electroweak symmetry. In the case of linear realization, the new physics is parameterized by higher dimension operators which contain the fields of the SM and are invariant under the SM symmetry, SM  $SU_c(3) \times SU_L(2) \times U_Y(1)$ .

Above the electroweak symmetry breaking scale but below the new physics scale, the effective Lagrangian can be written as

$$\mathcal{L}_{eff} = \mathcal{L}_0 + \frac{1}{\Lambda^2} \sum_i C_i O_i + O(\frac{1}{\Lambda^4}) \quad (1)$$

where  $\mathcal{L}_0$  is the SM Lagrangian,  $\Lambda$  is the new physics scale,  $O_i$  are dimension-six operators which are  $SU_c(3) \times SU_L(2) \times U_Y(1)$  invariant and  $C_i$  are constants which represent the coupling strengths of  $O_i$ . This expansion was first discussed in Ref.[6]. Recently the effective operators involving the top quark were reclassified and some are analyzed [7][8]. In this paper, we use such linearly realized effective Lagrangian and analyze all possible dimension-six CP-conserving operators containing anomalous  $Wtb$  couplings. For those operators which also give rise to anomalous  $Zb\bar{b}$  or right-handed  $Wtb$  couplings, we will examine their experimental constraints from the recent  $R_b$  data at LEP I and from the  $b \rightarrow s\gamma$  data at CLEO. Our analyses show that the existing experimental data strongly constrains the coupling strength of these operators. For other operators which subject to no strong experimental constraints so far, we find that the high energy  $e\gamma$  collider can provide an effective probe to their couplings.

This paper is organized as follows. In Sec. 2, we list the dimension-six operators which contribute to  $Wtb$  couplings. In Sec. 3 we derive the bounds from the data of  $R_b$  and  $b \rightarrow s\gamma$  for those which give rise to anomalous  $Zb\bar{b}$  coupling or right-handed  $Wtb$  coupling. In Sec. 4 we determine the possibility of probing anomalous  $Wtb$  coupling in the single top production at the high energy  $e\gamma$  collider. Finally, in Sec.5 we conclude our paper with discussions and a summary.

## 2. Operators contributing to $Wtb$ couplings

The dimension-six operators which contribute to the  $Wtb$  couplings are give by

$$O_{qW} = \left[ \bar{q}_L \gamma^\mu \tau^I D^\nu q_L + \overline{D^\nu q_L} \gamma^\mu \tau^I q_L \right] W_{\mu\nu}^I, \quad (2)$$

$$O_{\Phi q}^{(3)} = i \left[ \Phi^\dagger \tau^I D_\mu \Phi - (D_\mu \Phi)^\dagger \tau^I \Phi \right] \bar{q}_L \gamma^\mu \tau^I q_L, \quad (3)$$

$$O_{Db} = (\bar{q}_L D_\mu b_R) D^\mu \Phi + (D^\mu \Phi)^\dagger (\overline{D_\mu b_R} q_L), \quad (4)$$

$$O_{bW\Phi} = [(\bar{q}_L \sigma^{\mu\nu} \tau^I b_R) \Phi + \Phi^\dagger (\bar{b}_R \sigma^{\mu\nu} \tau^I q_L)] W^I, \quad (5)$$

$$O_{t3} = i [(\tilde{\Phi}^\dagger D_\mu \Phi) (\bar{t}_R \gamma^\mu b_R - (D_\mu \Phi)^\dagger \tilde{\Phi} (\bar{b}_R \gamma^\mu t_R)], \quad (6)$$

$$O_{Dt} = (\bar{q}_L D_\mu t_R) D^\mu \tilde{\Phi} + (D^\mu \tilde{\Phi})^\dagger (\overline{D_\mu t_R} q_L), \quad (7)$$

$$O_{tW\Phi} = [(\bar{q}_L \sigma^{\mu\nu} \tau^I t_R) \tilde{\Phi} + \tilde{\Phi}^\dagger (\bar{t}_R \sigma^{\mu\nu} \tau^I q_L)] W_{\mu\nu}^I, \quad (8)$$

where we follow the standard notation [7][8]:  $q_L$  denotes the third family left-handed doublet quarks,  $\Phi$  and  $\tilde{\Phi}$  are the Higgs field and its equivalent complex conjugate representation,  $W_{\mu\nu}$  and  $B_{\mu\nu}$  are the SU(2) and U(1) gauge boson field tensors in the appropriate matrix forms, and  $D_\mu$  denotes the appropriate covariant derivatives.

The expressions of these operators in the unitary gauge after electroweak symmetry breaking are given as

$$\begin{aligned} O_{qW} = & \frac{1}{2} W_{\mu\nu}^3 [\bar{t}_L \gamma^\mu \partial^\nu t_L + \partial^\nu \bar{t}_L \gamma^\mu t_L - \bar{b}_L \gamma^\mu \partial^\nu b_L - \partial^\nu \bar{b}_L \gamma^\mu b_L] \\ & + \frac{1}{\sqrt{2}} [W_{\mu\nu}^+ (\bar{t}_L \gamma^\mu \partial^\nu b_L + \partial^\nu \bar{t}_L \gamma^\mu b_L) + W_{\mu\nu}^- (\bar{b}_L \gamma^\mu \partial^\nu t_L + \partial^\nu \bar{b}_L \gamma^\mu t_L)] \\ & - i g_2 \bar{q}_L \gamma^\mu [W_\mu, W_\nu] \partial^\nu q_L - i g_2 \partial^\nu \bar{q}_L \gamma^\mu [W_\mu, W_\nu] q_L - i g_2 \bar{q}_L \gamma^\mu [W_{\mu\nu}, W^\nu] q_L, \end{aligned} \quad (9)$$

$$\begin{aligned} O_{\Phi q}^{(3)} = & -\frac{1}{2} g_Z (H + v)^2 Z_\mu [\bar{t}_L \gamma^\mu t_L - \bar{b}_L \gamma^\mu b_L] \\ & + \frac{1}{\sqrt{2}} g_2 (H + v)^2 [W_\mu^+ \bar{t}_L \gamma^\mu b_L + W_\mu^- \bar{b}_L \gamma^\mu t_L], \end{aligned} \quad (10)$$

$$\begin{aligned} O_{Db} = & \frac{1}{2\sqrt{2}} \partial^\mu H \left[ \partial_\mu (\bar{b}b) + \bar{b} \gamma_5 \partial_\mu b - (\partial_\mu \bar{b}) \gamma_5 b + \frac{2}{3} g_1 B_\mu \bar{b} i \gamma_5 b \right] \\ & + \frac{i}{4\sqrt{2}} g_Z (H + v) Z^\mu \left[ (\partial_\mu \bar{b}) b - \bar{b} \partial_\mu b - \partial_\mu (\bar{b} \gamma_5 b) - i \frac{2}{3} g_1 B_\mu (\bar{b}b) \right] \\ & - \frac{i}{2} g_2 (H + v) \left[ W_\mu^+ (\bar{t}_L \partial^\mu b_R + i \frac{g_1}{3} B^\mu \bar{t}_L b_R) - W_\mu^- (\partial^\mu \bar{b}_R t_L - i \frac{g_1}{3} B^\mu \bar{b}_R t_L) \right], \end{aligned} \quad (11)$$

$$\begin{aligned} O_{bW\Phi} = & \frac{1}{2} (H + v) \left[ W_{\mu\nu}^+ (\bar{t}_L \sigma^{\mu\nu} b_R) + W_{\mu\nu}^- (\bar{b}_R \sigma^{\mu\nu} t_L) - \frac{1}{\sqrt{2}} W_{\mu\nu}^3 (\bar{b} \sigma^{\mu\nu} b) \right. \\ & + i g_2 (W_\mu^+ W_\nu^3 - W_\mu^3 W_\nu^+) (\bar{t}_L \sigma^{\mu\nu} b_R) - i g_2 (W_\mu^- W_\nu^3 - W_\mu^3 W_\nu^-) (\bar{b}_R \sigma^{\mu\nu} t_L) \\ & \left. + i \frac{g_2}{\sqrt{2}} (W_\mu^+ W_\nu^- - W_\mu^- W_\nu^+) (\bar{b} \sigma^{\mu\nu} b) \right], \end{aligned} \quad (12)$$

$$O_{t3} = \frac{1}{2\sqrt{2}} g_2 (H + v)^2 [W_\mu^+ (\bar{t}_R \gamma^\mu b_R) + W_\mu^- (\bar{b}_R \gamma^\mu t_R)], \quad (13)$$

$$\begin{aligned}
O_{Dt} = & \frac{1}{2\sqrt{2}}\partial^\mu H \left[ \partial_\mu(\bar{t}t) + \bar{t}\gamma_5\partial_\mu t - (\partial_\mu\bar{t})\gamma_5 t - i\frac{4}{3}g_1 B_\mu\bar{t}\gamma_5 t \right] \\
& + i\frac{1}{4\sqrt{2}}g_Z(H+v)Z^\mu \left[ \bar{t}\partial_\mu t - (\partial_\mu\bar{t})t + \partial_\mu(\bar{t}\gamma_5 t) - i\frac{4}{3}g_1 B_\mu\bar{t}t \right] \\
& - i\frac{1}{2}g_2(H+v)W_\mu^- \left[ \bar{b}_L\partial^\mu t_R - i\frac{2}{3}g_1 B^\mu\bar{b}_L t_R \right] \\
& + i\frac{1}{2}g_2(H+v)W_\mu^+ \left[ (\partial^\mu\bar{t}_R)b_L + i\frac{2}{3}g_1 B^\mu\bar{t}_R b_L \right], \tag{14}
\end{aligned}$$

$$\begin{aligned}
O_{tW\Phi} = & \frac{1}{2\sqrt{2}}(H+v)(\bar{t}\sigma^{\mu\nu}t) \left[ W_{\mu\nu}^3 - ig_2(W_\mu^+W_\nu^- - W_\mu^-W_\nu^+) \right] \\
& + \frac{1}{2}(H+v)(\bar{b}_L\sigma^{\mu\nu}t_R) \left[ W_{\mu\nu}^- - ig_2(W_\mu^-W_\nu^3 - W_\mu^3W_\nu^-) \right] \\
& + \frac{1}{2}(H+v)(\bar{t}_R\sigma^{\mu\nu}b_L) \left[ W_{\mu\nu}^+ - ig_2(W_\mu^3W_\nu^+ - W_\mu^+W_\nu^3) \right], \tag{15}
\end{aligned}$$

where  $g_Z = 2m_Z/v = \sqrt{g_1^2 + g_2^2}$  with  $v$  being the vacuum expectation value of the Higgs boson.

The first four operators induce anomalous  $Zb\bar{b}$  couplings which will affect  $R_b$ . All operators contain an anomalous  $Wt\bar{b}$  coupling and the operator in Eq. (15) contains the  $Wt\bar{b}\gamma$  coupling. Both couplings contribute to the single top production at the  $e\gamma$  collider. The induced effective vertices for the couplings  $Zb\bar{b}$ ,  $Wt\bar{b}$  and  $Wt\bar{b}\gamma$  relevant to our analyses are given by

$$\begin{aligned}
\mathcal{L}_{Zb\bar{b}} = & \frac{C_{qW}}{\Lambda^2}\frac{c_W}{2}Z_{\mu\nu}(\bar{b}\gamma^\mu P_L\partial^\nu b + \partial^\nu\bar{b}\gamma^\mu P_L b) + \frac{C_{\Phi q}^{(3)}}{\Lambda^2}(vm_Z)Z_\mu(\bar{b}\gamma^\mu P_L b) \\
& + \frac{C_{Db}}{\Lambda^2}\frac{m_Z}{2\sqrt{2}}Z^\mu \left[ i(\partial_\mu\bar{b}b - \bar{b}\partial_\mu b) - i\partial_\mu(\bar{b}\gamma_5 b) \right] + \frac{C_{bW\Phi}}{\Lambda^2}\frac{c_W}{2}\frac{v}{\sqrt{2}}Z_{\mu\nu}(\bar{b}\sigma^{\mu\nu}b), \tag{16}
\end{aligned}$$

$$\begin{aligned}
\mathcal{L}_{Wt\bar{b}} = & \frac{C_{qW}}{\Lambda^2}\frac{1}{\sqrt{2}}W_{\mu\nu}^+(\bar{t}\gamma^\mu P_L\partial^\nu b + \partial^\nu\bar{t}\gamma^\mu P_L b) + \frac{C_{\Phi q}^{(3)}}{\Lambda^2}\frac{g_2}{\sqrt{2}}v^2W_\mu^+(\bar{t}\gamma^\mu P_L b) \\
& - \frac{C_{Db}}{\Lambda^2}\frac{v}{\sqrt{2}}\frac{g_2}{\sqrt{2}}W_\mu^+(i\bar{t}P_R\partial^\mu b) + \frac{C_{bW\Phi}}{\Lambda^2}\frac{v}{2}W_{\mu\nu}^+(\bar{t}\sigma^{\mu\nu}P_R b) \\
& + \frac{C_{t3}}{\Lambda^2}\frac{v^2}{2}\frac{g_2}{\sqrt{2}}W_\mu^+(\bar{t}\gamma^\mu P_R b) + \frac{C_{Dt}}{\Lambda^2}\frac{v}{\sqrt{2}}\frac{g_2}{\sqrt{2}}W_\mu^+(i\partial^\mu\bar{t})P_L b \\
& + \frac{C_{tW\Phi}}{\Lambda^2}\frac{v}{2}W_{\mu\nu}^+(\bar{t}\sigma^{\mu\nu}P_L b), \tag{17}
\end{aligned}$$

$$\mathcal{L}_{Wt\bar{b}\gamma} = \frac{C_{bW\Phi}}{\Lambda^2}(i2g_2s_W)W_\mu^+A_\nu(\bar{t}\sigma^{\mu\nu}P_R b), \tag{18}$$

where  $s_W \equiv \sin\theta_W$  and  $c_W \equiv \cos\theta_W$ .

### 3. Current bounds from experimental data

For the on-shell  $Z$ , we obtain the effective vertex  $Zb\bar{b}$

$$\Gamma_\mu = -i \frac{e}{4s_W c_W} \left[ \gamma_\mu V - \gamma_\mu \gamma_5 A + \frac{1}{2m_b} (p_b - p_{\bar{b}})_\mu S \right], \quad (19)$$

where  $p_b$  and  $p_{\bar{b}}$  are the momenta of outgoing quark and anti-quark, respectively. We write the vector and axial-vector couplings as

$$V = v_b + \delta V, \quad (20)$$

$$A = a_b + \delta A, \quad (21)$$

where  $v_b$  and  $a_b$  represent the SM couplings and  $\delta V, \delta A$  the new physics contributions. The SM couplings are given by

$$v_b = 2I_b^{3L} - 4s_W^2 e_b, \quad (22)$$

$$a_b = 2I_b^{3L}, \quad (23)$$

where  $e_b = -1/3$  is the electric charge and  $I_b^{3L} = -1/2$  the weak isospin of the  $b$  quark. The new physics contributions  $\delta V$  and  $\delta A$  are given by

$$\delta V = \delta A = \frac{2s_W c_W}{e} \frac{vm_Z}{\Lambda^2} \left[ C_{qW} \frac{c_W m_Z}{2v} - C_{\Phi q}^{(3)} \right], \quad (24)$$

$$S = -\frac{8s_W c_W}{e} \frac{m_b}{\Lambda^2} \frac{v}{\sqrt{2}} \left[ C_{Db} \frac{m_Z}{2v} - C_{bW\Phi} c_W \right]. \quad (25)$$

In terms of the vertices given in Eq.(19), the observable  $R_b$  at LEP I is given by, to the order of  $\frac{1}{\Lambda^2}$ ,

$$R_b = R_b^{SM} \left[ 1 + 2 \frac{v_b \delta V + a_b \delta A}{v_b^2 + a_b^2} (1 - R_b^{SM}) \right], \quad (26)$$

where we have neglected the bottom quark mass. Thus we have

$$\delta V = \delta A = \frac{R_b^{exp} - R_b^{SM}}{(1 - R_b^{SM}) R_b^{SM}} \frac{v_b^2 + a_b^2}{2(v_b + a_b)}. \quad (27)$$

The SM values on  $R_b$  and the latest experimental data are [5]

$$R_b^{SM} = 0.2158, \quad R_b^{exp} = 0.2170(9). \quad (28)$$

From Eq.(27) and Eq.(28), we obtain at the  $1\sigma$  ( $3\sigma$ ) level

$$-0.0053 \text{ } (-0.01) < \delta V < -0.0007 \text{ } (0.004). \quad (29)$$

Assuming that no cancellation between  $O_{qW}$  and  $O_{\Phi q}^{(3)}$  occurs, we obtain the bound for each of them at the  $1\sigma$  ( $3\sigma$ ) level

$$-0.5 \text{ } (-1.03) < \frac{C_{qW}}{(\Lambda/\text{TeV})^2} < -0.07 \text{ } (0.41), \quad (30)$$

$$0.01 \text{ } (-0.07) < \frac{C_{\Phi q}^{(3)}}{(\Lambda/\text{TeV})^2} < 0.09 \text{ } (0.17). \quad (31)$$

Since the operators  $O_{bW\Phi}$  and  $O_{Db}$  only appear in the  $S$  factor in Eq. (25), their contributions to  $R_b$  at LEP I are proportional to  $m_b/m_Z$  and hence suppressed. Therefore, they are not constrained by  $R_b$  at LEP I. However, as Eq. (17) shows,  $O_{bW\Phi}$  induces a right-handed weak charged current, and thus it will be constrained by the CLEO measurement on  $b \rightarrow s\gamma$  [9]. The latest limit can be found in Ref. [10], i.e.,

$$-0.03 < \frac{C_{bW\Phi}}{\Lambda^2} \frac{\sqrt{2}vm_t}{g_2} < 0.00, \quad (32)$$

which gives

$$-0.3 < \frac{C_{bW\Phi}}{(\Lambda/\text{TeV})^2} < 0. \quad (33)$$

For  $O_{t3}$ ,  $O_{Dt}$  and  $O_{tW\Phi}$ , they are not constrained by  $R_b$  at the tree level. However, at one-loop level they contribute to gauge boson self-energies, and thus rather loose bounds exist [7] with significant uncertainties. However more reliable, but still rather weak, bounds for them can be obtained from the unitarity bound [7]. For  $\Lambda = 1 \text{ TeV}$ , the unitarity bounds are given by [7]

$$|C_{t3}| < 61.5, \quad |C_{Dt}| < 10.4, \quad |C_{tW\Phi}| < 13.5. \quad (34)$$

## 4. Effects on single top quark production at $e\gamma$ colliders

Now we examine the effects of the operators in Eqs. (2)-(8) in the single top production at high energy  $e\gamma$  colliders. The tree diagrams are depicted in Fig. 1. We note that the effects of  $O_{qW}$  is  $q^2$ -dependent and it can be enhanced with higher collider energy. Since the other operators are momentum independent, they do not have the energy enhancement effect. Therefore,  $O_{qW}$  is of special interest and we will present its treatment in some detail. For the other operators we will only present the resultant upper bounds we obtained on their couplings that can be probed at the  $e\gamma$  collider.

## 4.1 Effects of $O_{qW}$

With the effective coupling given in Eqs.(17) and (18), the relevant Feynman rules, Feynman diagrams, and Feynman amplitudes are implemented in our program package FDC97 [11]. We take  $m_t=175$  GeV,  $m_b=4.3$  GeV,  $\alpha_{EW}(m_Z)=1/128$ ,  $|V_{tb}|=0.9984$ ,  $m_Z=91.187$  GeV,  $\sin^2 \theta_W=0.232$ ,  $m_W=m_Z \cos \theta_W$ ,  $\Gamma_Z=2.50$  GeV and  $\Gamma_W=2.09$  GeV.

For  $O_{qW}$ , the coupling strength  $C_{qW}/\Lambda^2$  can be determined from Eqs.(26) and (24), as a function of  $R_b$ . In order to show the effect of the constraint from the experimental value of  $R_b$ , it will be interesting to investigate the contribution of  $O_{qW}$  to the cross section and the luminosity required to observe the effect of  $O_{qW}$  as a function of  $R_b$ .

The center-of-mass energy of the  $e\gamma$  is determined by that of the  $e^+e^-$  collider in which one of the lepton beams, say that of the  $e^+$ , is back-scattered from a laser beam to produce the high energy photon beam. Hence, the photon beam so produced falls into a spectrum of energies for a given beam of  $e^+$  energy. We refer to Ref. [12] for the details of the photon beam energy spectrum. The measurable cross section for the reaction  $e\gamma \rightarrow \bar{t}b\nu$  is a convolution of the reaction cross section at fixed energy with the photon energy spectrum. As the photon energy spectrum is completely determined by the center-of-mass energy of the  $e^+e^-$  collider  $E_{e^+e^-}$  [12], we will use the latter to represent the effective center-of-mass energy of the  $e\gamma$  collider.

In Fig. 2, we show the contribution of  $O_{qW}$  to the total cross section of the single top production as a function of  $R_b$ . The solid and dashed curves are for  $E_{e^+e^-} = 500$  GeV and

1 TeV, respectively. One can see that the experimental data on  $R_b$ , i.e.,  $R_b^{exp} = 0.2170(9)$ , has severely constrained the contributions of  $O_{qW}$  to the single top production rate. For example, with  $R_b$  varied within  $2\sigma$ , i.e.,  $0.2152 < R_b < 0.2188$ , the contribution of  $O_{qW}$  to the single top rate of the SM prediction is limited to be less than 8% and 4% for  $E_{e^+e^-} = 1$  TeV and 500 GeV, respectively.

As we pointed out earlier, since the effects of  $O_{qW}$  is  $q^2$ -dependent, its effects will be enhanced as the collider energy increases. In Fig. 3 we plot the total cross sections of single top production, with and without the contribution of  $O_{qW}$ , as a function of center-of-mass energy. Here we see that the effects of  $O_{qW}$  are enhanced significantly when the center-of-mass energy is above 1 TeV.

The existence of  $O_{qW}$  will also affect the distribution properties of the final state particles. In Fig.4, we plotted three distributions,  $d\sigma/d\cos\Theta_{\gamma b}$ ,  $d\sigma/dp_t^T$  and  $d\sigma/dp_b^T$ . Here  $\theta_{\gamma b}$  is the angle of the  $b$ -quark with respect to the incident photon direction in the  $e^+e^-$  rest frame, and  $p_t^T$  and  $p_b^T$  are transverse momentum of  $\bar{t}$  and  $b$  quarks, respectively. These figures also show that the new physics contribution can be enhanced relative to the SM prediction if appropriate cuts on the transverse momentum and the angle are imposed. We found the optimal cuts to be

$$\cos\theta_{\gamma b} \leq 0.84, \quad p_t^T \geq 70\text{GeV}, \quad p_b^T \geq 30\text{GeV}. \quad (35)$$

To estimate the luminosity required for observing the effects of  $O_{qW}$ , we define the significance of the signal relative to the background in terms of Gaussian statistics, in which a signal at the 99% CL is defined by

$$S \geq 3\sqrt{S+B}, \quad (36)$$

where  $S$  and  $B$  are the number of signal and background events. Applying the cuts of Eq.(35), we obtain the luminosity required for observing the effects of  $O_{qW}$  at 99% C.L. as a function of  $R_b$ . This is shown in Fig.5, where the solid and dashed curves are for 100% and 30% of detection efficiency, respectively. The upper (lower) curves correspond to negative (positive) values of  $C_{qW}/\Lambda^2$ . One can see that if  $R_b$  is constrained within  $2\sigma$  of the

experimental value, the required integrated luminosity is  $4 \text{ fb}^{-1}$  ( $20 \text{ fb}^{-1}$ ) for 100% (30%) of detection efficiency. For a 1 TeV  $e\gamma$  collider with  $L = 10 \text{ fb}^{-1}$  and 30% detection efficiency, the absence of an anomalous top quark production will set a bound

$$-0.85 < \frac{C_{qW}}{(\Lambda/\text{TeV})^2} < 0.38, \quad (37)$$

which is slightly stronger than the corresponding  $3\sigma$  bound from  $R_b$  as given in Eq.(30).

## 4.2 Effects of $O_{\Phi q}^{(3)}$ , $O_{bW\Phi}$ , $O_{Db}$ , $O_{t3}$ , $O_{Dt}$ and $O_{tW\Phi}$

The effects of these operators can be analyzed similar to that of  $O_{qW}$  but they are momentum independent and thus cannot be enhanced when the collider energy increases. Here we only present the results of our calculation on the upper bounds of each of them by assuming the existence of one operator at a time. For  $E_{e^+e^-} = 1 \text{ TeV}$ ,  $L = 10 \text{ fb}^{-1}$  and a detection efficiency of 30%, they are given by, at 99% C.L.,

$$-1.9 < \frac{C_{\Phi q}^{(3)}}{(\Lambda/\text{TeV})^2} < 2.1, \quad (38)$$

$$-0.40 < \frac{C_{bW\Phi}}{(\Lambda/\text{TeV})^2} < 0.80, \quad (39)$$

$$-11.8 < \frac{C_{Db}}{(\Lambda/\text{TeV})^2} < 15.0, \quad (40)$$

$$-18.5 < \frac{C_{t3}}{(\Lambda/\text{TeV})^2} < 12.8, \quad (41)$$

$$-4.2 < \frac{C_{Dt}}{(\Lambda/\text{TeV})^2} < 4.0, \quad (42)$$

$$-0.65 < \frac{C_{tW\Phi}}{(\Lambda/\text{TeV})^2} < 0.46. \quad (43)$$

We note the bounds on  $O_{\Phi q}^{(3)}$  and  $O_{bW\Phi}$  are also weaker than the current ones set by  $R_b$  and  $b \rightarrow s\gamma$  as given in (31) and (33). For  $O_{t3}$ ,  $O_{Dt}$  and  $O_{tW\Phi}$ , these bounds are much stronger than their corresponding unitarity bounds which are given by [7] and quoted in Eq. (34).

## 5. Discussion and summary

In our analyses we assumed the existence of one operator at one time. However, if they coexist, their effects have to be disentangled in a degree by analyzing additional measurable quantities and by examining how all the measurable quantities change under the variation of the couplings of the operators involved as shown in Ref. [13] and [14]. Such detailed analyses are not warranted at the present time and we will be content ourselves by a few pertinent remarks:

(1) The contribution of  $O_{qW}$  is momentum dependent and thus the behavior of the cross section versus  $E_{e^+e^-}$  is different from that predicted by the SM, as shown in Fig. 3. So we can disentangle the effects of  $O_{qW}$  from the behavior of the cross section versus  $E_{e^+e^-}$ .

(2) Since the effects of other operators,  $O_{\Phi q}$ ,  $O_{bW\Phi}$ ,  $O_{Db}$ ,  $O_{t3}$ ,  $O_{Dt}$  and  $O_{tW\Phi}$ , are momentum independent, the behavior of the cross section with their contribution versus  $\sqrt{s}$  is the same as that predicted by the SM. Thus it is hard to distinguish one from another among these operators. However, the effects of  $O_{\Phi q}$  and  $O_{bW\Phi}$ , which subject to similar current constraints as  $O_{qW}$ , have limited effects at  $e\gamma$  colliders. If the new physics effects at  $e\gamma$  colliders are found to be larger than such limited effects presented in Figs. 2-4, we could say they may arise from  $O_{Db}$ ,  $O_{t3}$ ,  $O_{Dt}$  or  $O_{tW\Phi}$  and more detailed study of these operators are necessary.

To summarize, we used the effective Lagrangian approach to the new physics of the top quark to study the possibility of observing anomalous  $Wtb$  couplings in the single top production at a high energy  $e\gamma$  collider. Our results indicate that a luminosity of the order of  $100\text{ fb}^{-1}$  is needed to reveal the effects of those operators which are subjected to the stringent constraints obtained from  $R_b$  and  $b \rightarrow s\gamma$ . For the operators which are not subjected to any bounds presently, meaningful limits of their couplings can be obtained at a  $e\gamma$  collider.

## Acknowledgement

We would like to thank E. Boos for discussions. J. M. Y. acknowledges JSPS for the Postdoctoral Fellowship. This work was supported in part by the U.S. Department of Energy, Division of High Energy Physics, under Grant No. DE-FG02-94ER40817, by the

National Natural Science Foundation of China, and by the Grant-in-Aid for JSPS fellows from the Japan Ministry of Education, Science, Sports and Culture.

## References

- [1] R.D. Peccei and X. Zhang, Nucl. Phys. B337, 269 (1990); R.D. Peccei, S. Peris and X. Zhang, Nucl. Phys. B349, 305 (1991); X. Zhang and B.-L. Young, Phys. Rev. D51, 6564 (1995).
- [2] C.T. Hill and S. Parke, Phys. Rev. D49, 4454 (1994); D. Atwood, A. Kagan and T. Rizzo, Phys. Rev. D52, 6264 (1995); D.O. Carlson, E. Malkawi and C.-P. Yuan, Phys. Lett. B337, 145 (1994); H. Georgi, L. Kaplan, D. Morin and A. Shenk, Phys. Rev. D51, 3888 (1995); T. Han, R. D. Peccei and X. Zhang, Nucl. Phys. B454, 527 (1995); K. Cheung, Phys. Rev. D53, 3604 (1996); E. Malkawi and T. Tait, Phys. Rev. D54, 5758 (1996); S. Dawson and G. Valencia, Phys. Rev. D53, 1721 (1996); T. G. Rizzo, Phys. Rev. D53, 6218 (1996); P. Haberl, O. Nachtman and A. Wilch, Phys. Rev. D53, 4875 (1996); T. Han, K. Whisnant and B.-L. Young and X. Zhang, Phys. Lett. B385, 311 (1996); G. J. Gounaris, M. Kuroda and F.M. Renard, Phys. Rev. D54, 6861 (1996); G. J. Gounaris, J. Layssac and F. M. Renard, Phys. Rev. D55, 5786 (1997); G. J. Gounaris, J. Layssac, D.T. Papadamou, G. Tsirigoti and F.M. Renard, hep-ph/9708204; G. J. Gounaris, D. T. Papadamou and F. M. Renard, hep-ph/9711399. K. Cheung, Phys. Rev. D55, 4430 (1997).
- [3] G. Jikia, Nucl. Phys. B374, 83 (1992); E. Boos, Y. Kurihara, Y. Shimizu, M. Sachwitz, H. J. Schreiber and S. Shichanin, Z. Phys. C70, 255 (1996); E. Boos, A. Pukhov, M. Sachwitz and H. J. Schreiber, Z. Phys. C75, 237 (1997).
- [4] E. Boos, A. Pukhov, M. Sachwitz, H. J. Schreiber Phys. Lett. B404, 119 (1997).
- [5] G. Alteralli, CERN-TH-97-278, hep-ph/9710434.

- [6] C. J. C. Burgess and H. J. Schnitzer, Nucl. Phys. B228, 454 (1983);  
C. N. Leung, S. T. Love and S. Rao, Z. Phys. C31, 433 (1986); W. Buchmuller and D. Wyler, Nucl. Phys. B268, 621 (1986).
- [7] G. J. Gounaris, F. M. Renard and C. Verzegnassi, Phys. Rev. D52, 451 (1995); G. J. Gounaris, D. T. Papadamou and F. M. Renard, Z. Phys. C76, 333 (1997);
- [8] K. Whisnant, J. M. Yang, B.-L. Young and X. Zhang, Phys. Rev. D56, 467 (1997); J. M. Yang and B.-L. Young, Phys. Rev. D56, 5907 (1997);
- [9] M. Alam et al., CLEO Collaboration, Phys. Rev. Lett. 74, 2885 (1995).
- [10] M. Hosch, K. Whisnant and B.-L. Young, Phys. Rev. D55, 3137 (1997).
- [11] J.-X. Wang, Computer Phys. Commun. 86 (1993) 214-231;  
J.-X. Wang, preprint KEK-TH-412, 1993, Proceeding of AI93, Oberamergau, Germany;  
J.-X. Wang, Proceeding of AI96, Sept. 1996, Lausanne, Switzerland.
- [12] K. Cheung, S. Dawson, T. Han, and G. Valencia, Phys. Rev. D51, 5 (1995).
- [13] A. Datta, K. Whisnant, Bing-Lin Young and X. Zhang, Phys. Rev. D57, 346 (1997).
- [14] K. Hikasa, K. Whisnant, J. M. Yang and B.-L. Young, hep-ph/9806401.

## Figure Captions

Fig.1 Feynman diagrams for  $\gamma e \rightarrow \nu t \bar{b}$ .

Fig.2 The ratio of  $\Delta\sigma/\sigma_{SM}$  for the reaction  $\gamma e \rightarrow \nu t \bar{b}$  versus  $R_b$ , where  $\Delta\sigma = \sigma - \sigma_{SM}$  with  $\sigma$  and  $\sigma_{SM}$  being the cross section with and without the contribution of  $O_{qW}$ , respectively. The solid (dashed) curve is for  $E_{e^+e^-} = 500$  (1000) GeV.

Fig.3 Cross section of reaction  $\gamma e \rightarrow \nu t \bar{b}$  as a function of  $E_{e^+e^-}$ . The thin line represents SM expectations, while the dashed and thick lines are the results with the contribution of  $O_{qW}$  for  $R_b = 0.2152$  and  $R_b = 0.2188$ , respectively.

Fig.4 The distribution of differential cross section of the reaction  $\gamma e \rightarrow \nu t \bar{b}$  versus  $\cos\theta_{\gamma b}$ ,  $p_t^T$  and  $p_b^T$ . The thick and thin lines represent the SM predictions and the predictions with the contribution of  $O_{qW}$  for  $R_b = 0.2188$ , respectively.

Fig.5 The luminosity required to detect the effects of  $O_{qW}$  at 99% CL as a function of  $R_b$ . The solid (dashed) curves are for 100% (30%) of event detection efficiency.

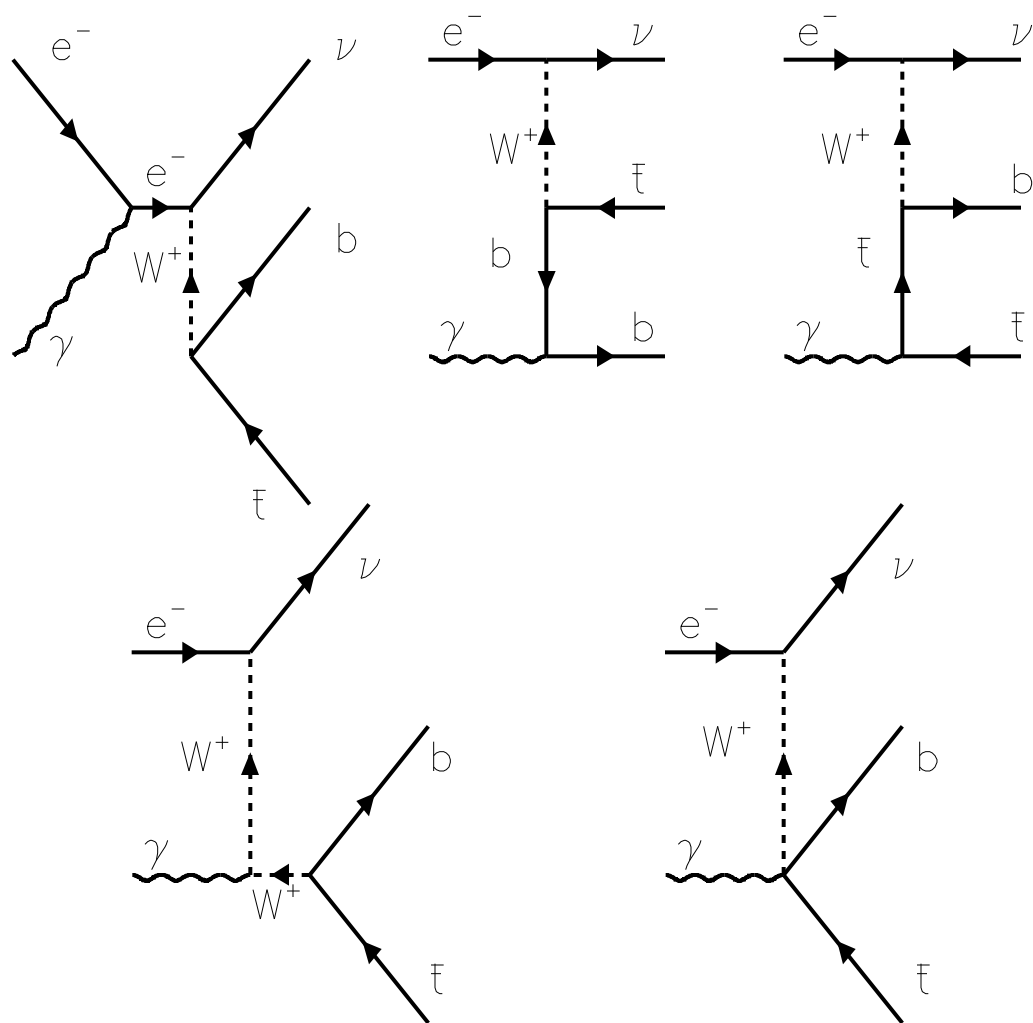
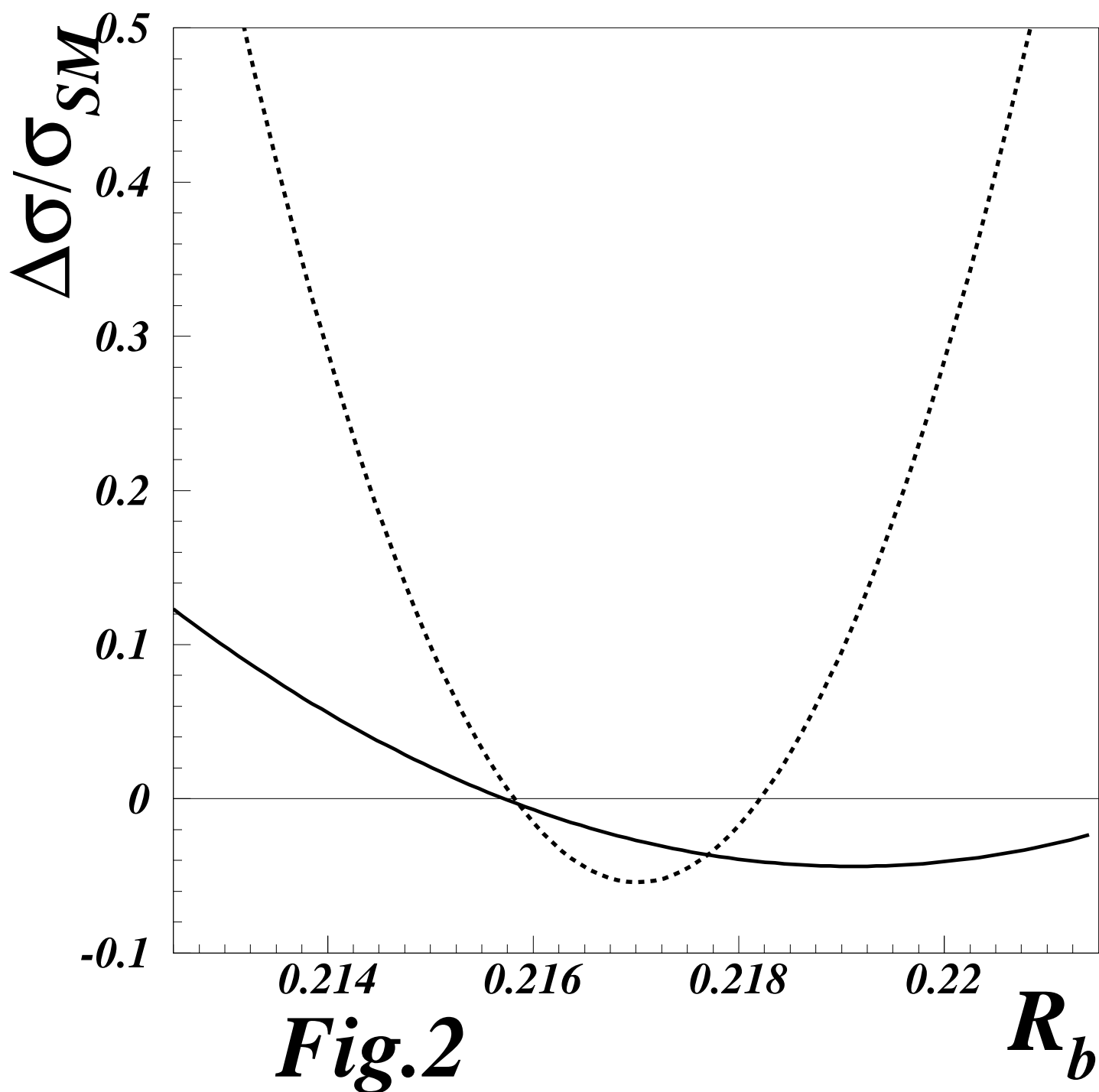
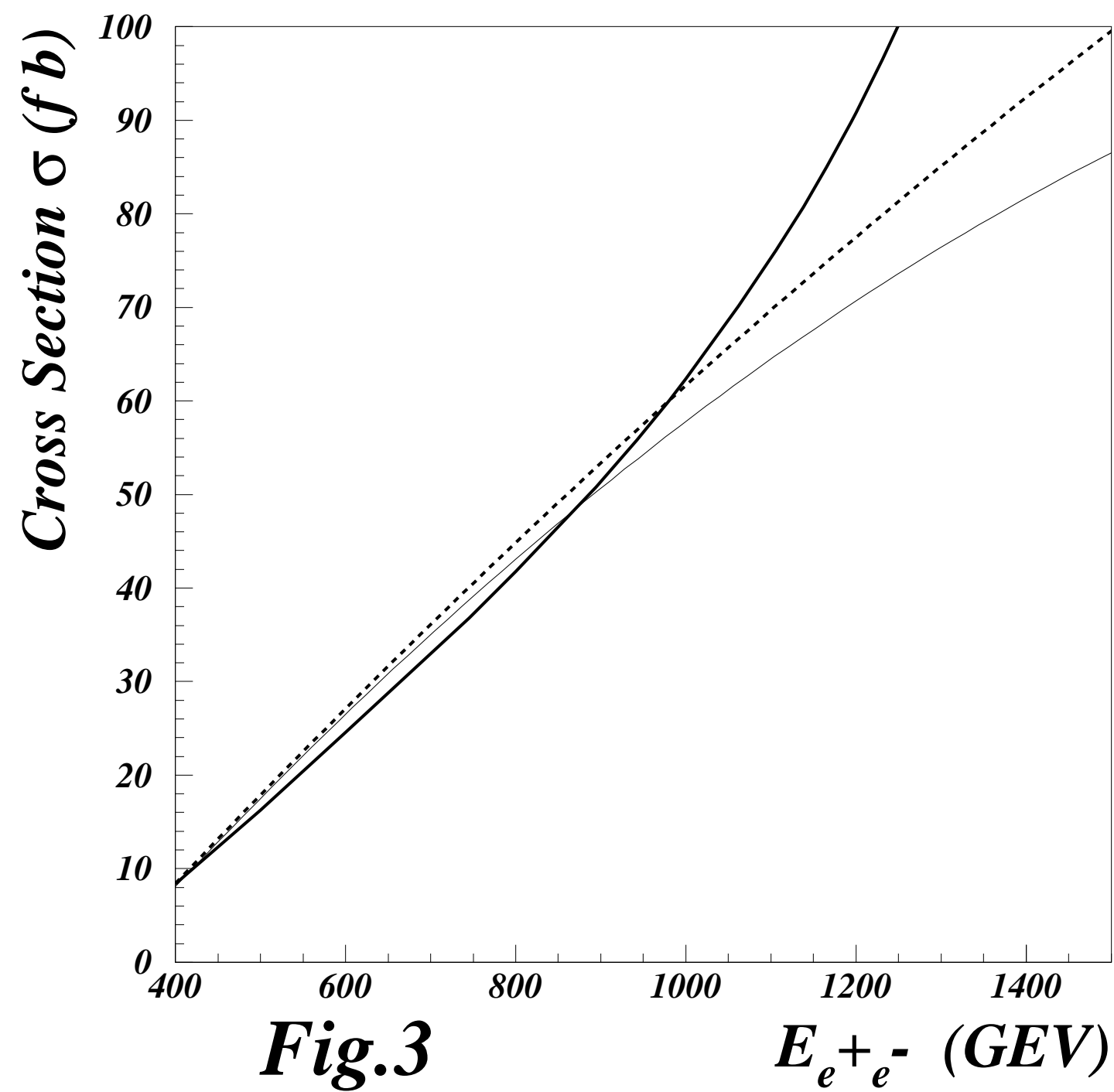
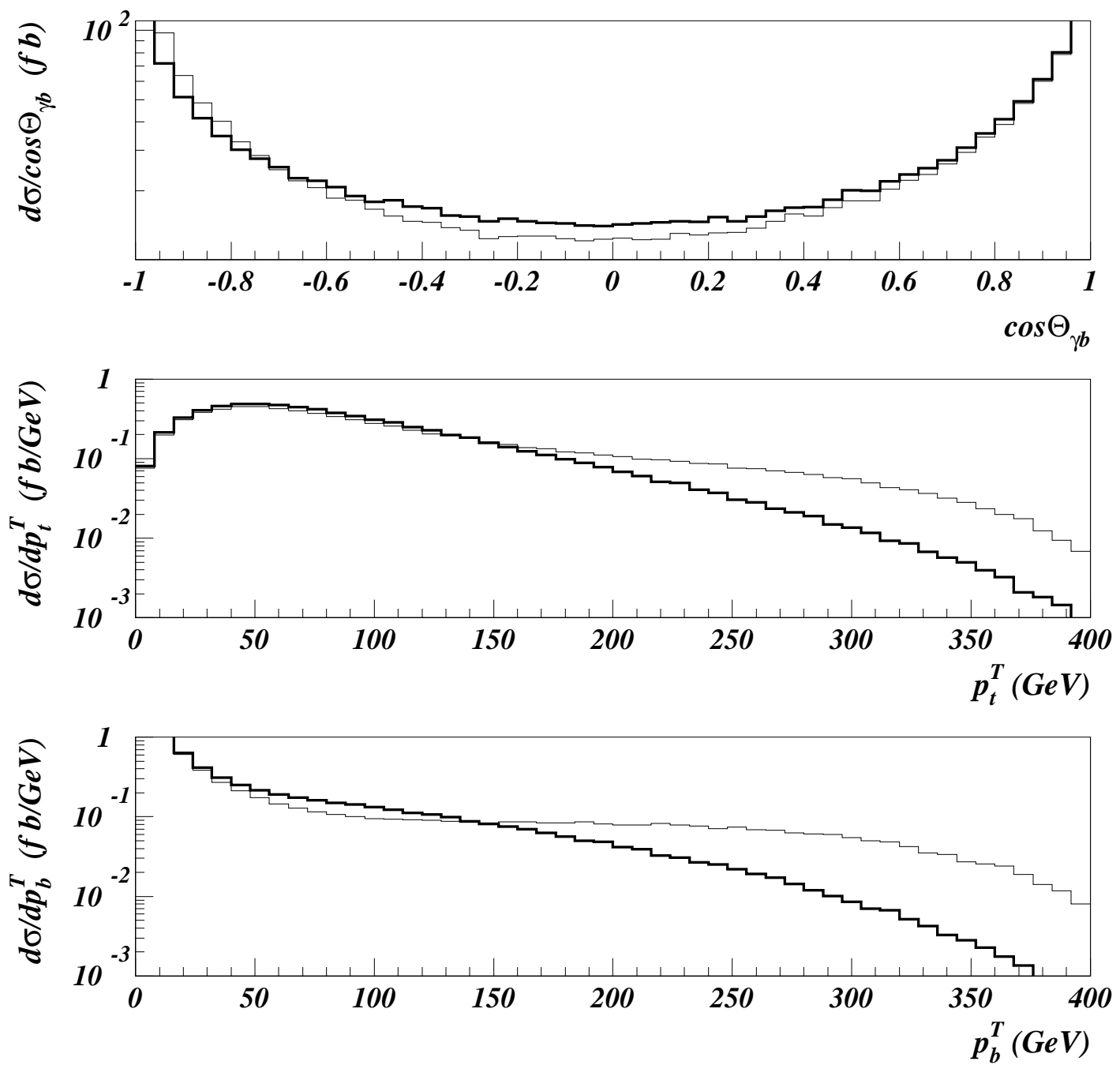


Fig.1







***Fig.4***

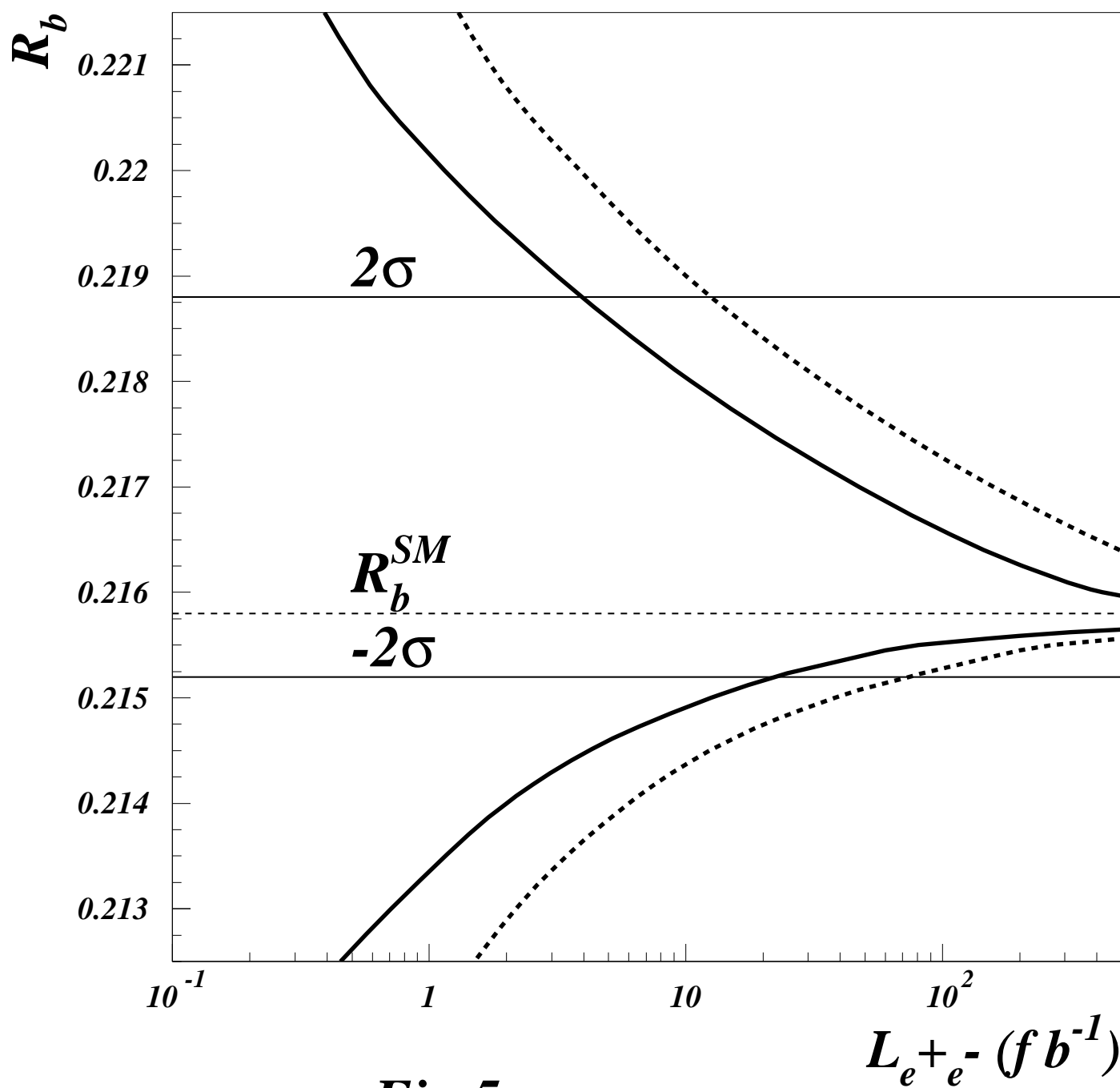


**Fig.5**